stress time. The average D_{it} values as a function of log stress time for the same three devices are shown in Fig. 3, again with the 'PRE' value included. The observed increase in D_{it} with stress time agrees with previously published results [5].

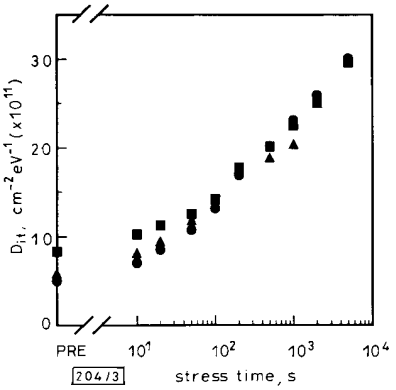

Fig. 3 *D_{it} against loss stress time*

● device 1
▲ device 2
■ device 3

Relating shifts or increases in K to D_{it} provides an easy way to directly compare the data of Figs. 2 and 3. In Fig. 4, the increase in the noise constant K is plotted as a function of the increase in average D_{it}. As can be seen, K and D_{it} increase in direct proportion during the high field stressing.

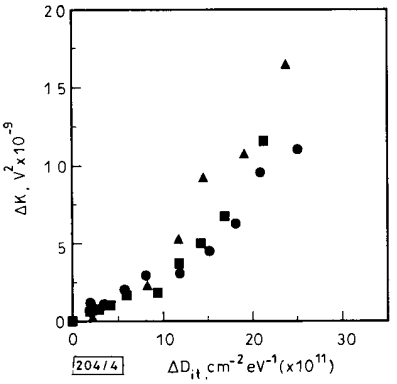

Fig. 4 *Increase in noise constant K against increase in D_{it}*

● device 1
▲ device 2
■ device 3

Conclusions: For *p*MOS transistors subjected to high field stress, a direct relationship between the increase in linear region $1/f$ noise and D_{it} is observed. This correlation during high field stressing is in agreement with measurements previously performed on differently processed devices and devices subjected to ionising radiation [1–3].

Acknowledgments: The authors would like to thank H. Parks and B. Craigin of the University of Arizona for useful discussions and D. Wayne, G. Harder and P. Gerrish of Micro-Rel in Tempe, AZ, for their help in packaging the transistors. This work has been supported in part by the Defense Nuclear Agency through contract number DNA001-92-C-0022.

4th March 1993

J. L. Todsen,* P. Augier,† R. D. Schrimpf and K. F. Galloway (*Department of Electrical and Computer Engineering, University of Arizona, Tucson, AZ 85719, USA*)

* Now at IBM, Tucson, AZ 85744, USA
† Visiting scholar from the University of Montpellier II, Montpellier, France

References

1 KLAASSEN, F. M.: 'Characterisation of low $1/f$ noise in MOS transistors', *IEEE Trans.*, 1971, **ED-18**, pp. 887–891
2 BROUX, G., VAN OVERSTRAETEN, R. J., and DECLERCK, G. J.: 'Experimental results on fast surface states and $1/f$ noise in MOS transistors', *Electron. Lett.*, 1975, **11**, pp. 97–98
3 AUGIER, P., TODSEN, J. L., ZUPAC, D., SCHRIMPF, R. D., GALLOWAY, K. F., and BABCOCK, J. A.: 'Comparison of $1/f$ noise in irradiated power MOSFETs measured in the linear and saturation regions', *IEEE Trans.*, 1992, **NS-39**
4 LENZLINGER, M., and SNOW, E. H.: 'Fowler–Nordheim tunneling into thermally grown SiO_2', *J. Appl. Phys.*, 1969, **40**, pp. 278–283
5 LIANG, M.-S., CHANG, C., YEOW, Y. T., HU, C., and BRODERSEN, R. W.: 'MOSFET degradation due to stressing of thin oxides', *IEEE Trans.*, 1984, **ED-31**, pp. 1238–1244
6 CHRISTENSSON, S., LUNDSTROM, I., and SVENSSON, C.: 'Low frequency noise in MOS transistors—I. Theory', *Solid-State Electron.*, 1968, **11**, pp. 797–812
7 BLASQUEZ, G., and BOUKABACHE, A.: 'Origins of $1/f$ noise in MOS transistors', *in* SAVELLI, M., LECOY, G., and NOUGIER, J.-P. (Eds.): 'Physical systems and $1/f$ noise' (Elsevier Science Publishers B.V., Amsterdam, 1983)
8 MEISENHEIMER, T. L., and FLEETWOOD, D. M.: 'Effects of radiation-induced charge on $1/f$ noise in MOS devices', *IEEE Trans.*, 1990, **NS-37**, pp. 1696–1702
9 MCWHORTER, A. L.: '$1/f$ noise and germanium surface properties', *in* 'Semiconductor surface physics' (University Press, Philadelphia, 1957)
10 GROESENEKEN, G., MAES, H. E., BELTRAN, N., and DE KEERSMAECKER, R. F.: 'A reliable approach to charge-pumping measurements in MOS transistors', *IEEE Trans.*, 1984, **ED-31**, pp. 42–53

PRMA EFFICIENCY IN ADAPTIVE TRANSCEIVERS

L. Hanzo, J. C. S. Cheung and R. Steele

Indexing terms: Transceivers, Signal processing, Adaptive systems

The effects of different speech source rates and various number of modulation levels on packet reservation multiple access (PRMA) efficiency in an adaptive transceiver are investigated under the constraint of fixed channel bandwidth and benign cochannel interference in office type cordless telecommunications (CT) environments. The number of PRMA users supported in a 200 kHz frequency slot ranges from 17 to 103, the required user bandwidth is between 11·8 and 1·94 kHz, and the number of PRMA users per slot is between 1·7 and 1·94, respectively.

Introduction: It is envisaged that in intelligent third generation personal communications networks (PCN) the transceivers can adaptively reconfigure themselves in order to meet time-varying optimisation criteria.* In this Letter the effect of using packet reservation multiple access (PRMA) in conjunction with adaptive transceivers incorporating full-rate, half-rate and quarter-rate speech codecs as well as 1, 2 and 4 bit/symbol modulation schemes is investigated.

System description: We focus our experiments on an adaptive cordless telecommunications (CT) transceiver, where the modulated signal fits in a 200 kHz channel slot used in the Pan-European mobile radio system, known as GSM. The full-rate speech source codec generates a 260 bit/20 ms = 13 kbit/s information stream, which is channel coded to 456 bit/20 ms = 22·8 kbit/s. However, instead of the complex GSM control infrastructure [2] here we opt for a low-delay, low-complexity control scheme using a 64 bit header, favoured in office-type CT schemes [2]. With this 64 bit header the source information rate becomes (456 + 64) bits per 20 ms, i.e. 520 bit/20 ms = 26 kbit/s. Similarly, the half-rate codec generates (228 + 64) = 292 channel coded bits per 20 ms, yielding a

* WILLIAMS, J., HANZO, L., STEELE, R., and CHEUNG, J. C. S.: 'On the performance of adaptive speech terminals for UMTS'. Unpublished

source rate of 14·6 kbit/s. Lastly, the future quarter-rate source and channel codec will produce (114 + 64) = 178 bits per 20 ms, which is equivalent to a PRMA source rate of 8·9 kbit/s. These values are listed in columns 3 and 4 of Table 1. The GSM modulation scheme is binary Gaussian minimum shift keying (GMSK), as seen for systems A–C in column 2.

Apart from reducing the speech source rate, the user bandwidth can also be reduced by deploying multilevel modems using 2 or 4 bit/symbol transmissions. This approach has been favoured in the American and Japanese second generation digital mobile radio systems, where a 2 bit/symbol $\pi/4$-shifted differential quadrature phase shift keying ($\pi/4$-DQPSK) modem is proposed. Systems D-F are based on $\pi/4$-DQPSK modems combined with the previous three speech codecs. In office environments, where high signal to noise ratio (SNRs), low dispersion and benign cochannel interference prevail we have had encouraging experience with 16 level star-constellation quadrature amplitude modulation (16-StQAM) [3]. Hence in systems G–J we used 16-StQAM. The important related issues of linear amplification or pre- and postdistortion have been considered in Reference 4. The typically lower cochannel interference tolerance of multilevel modulation is mitigated by the partitioning walls, which naturally curtail interference in indoor CT schemes. Intersymbol interferences are mitigated by using smooth raised cosine Nyquist filtering with a rolloff factor of 0·35 for $\pi/4$-DQPSK and 1 for 16-StQAM, while adjacent channel interference can be reduced using appropriate guard bands. As a consequence, the channel occupancy gains of the multilevel schemes have to be moderated by their stringent filtering requirements. Defining the bandwidth as the point where the modulated spectrum decayed by 24 dB for $\pi/4$-DQPSK and 16-StQAM, their bandwidth efficiencies are 1·62 bit/Hz and 2·4 bit/Hz, respectively [1]. Therefore the signalling rates accommodated within the 200 kHz GSM channel slot are 162 kbaud and 120 kbaud, respectively, whereas for GMSK the standard 270 kbaud GSM rate is used. From these TDMA burst rates and the PRMA source symbol rates of column 4 the number of time division multiple access (TDMA) slots accommodated is calculated by division. These values are listed in column 6 of Table 1, and the corresponding TDMA user bandwidths are summarised in column 5 of Table 1, which are also derived by straightforward division. PRMA is an efficient multiplexing method for organising the flow of speech packets via TDMA systems [5]. It improves the bandwidth efficiency of all proposed TDMA schemes significantly by surrendering inactive TDMA time slots to those users who are becoming active, a process controlled by the PRMA multiplexer at the base station (BS). Users queue their speech packets to contend for a specific free time slot only if the VAD [6] detects an active speech spurt and they were granted permission to contend. Colliding users are allowed to content for consecutive available time slots only with a permission probability less than unity to prevent them from consistently colliding in their further attempts to attain a slot reservation. The optimum permission probability P_{perm} is inversely proportional to the number of TDMA time slots available [5] and the values used in our schemes are listed in column 10 of Table 1. Should only one user require a free time slot, he can reserve it for future use until he no longer has packets to transmit. If, however, several users contend for a reservation, collision takes place and neither of them will be granted it. When numerous users are contending for a reservation, a speech packet might consistently collide with others and should the contention delay exceed 32 ms, the speech packet of 20 ms duration must be dropped. However, $P_{drop} < 1\%$ must be maintained to minimise speech impairments.

Results and discussion: The PRMA schemes of systems A–J were simulated and their packet dropping probability against number of users curves are plotted in Fig. 1. The number of users supported at $P_{drop} = 1\%$ as seen from Fig. 1 is tabulated in column 7 of Table 1. Dividing these values with the number of TDMA time slots gives the relative number of PRMA users per slot, as summarised in column 8, which is an important PRMA efficiency indicator for our systems. Dividing the bandwidth of 200 kHz by the number PRMA users yields the PRMA user channel occupancy values listed in column 9 of Table 1.

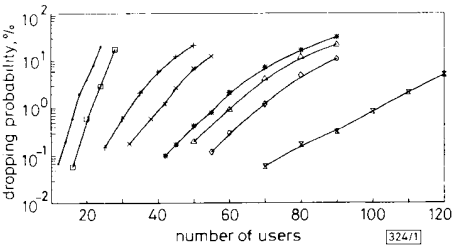

Fig. 1 *PRMA packet dropping probability against number of users for GSM-type systems*

- A, 10 slots
- B, G, 18 slots
- C, 30 slots
- D, 12 slots
- E, 22 slots
- F, 36 slots
- H, 32 slots
- J, 53 slots

Observe the general trend that lower speech source rates or higher numbers of source bits per modulation symbol allow for more time slots to be created and this in turn improves the PRMA efficiency, as demonstrated by column 8 of Table 1. It is also more beneficial in terms of both PRMA efficiency and equipment complexity to opt for doubling the number of bits per modulation symbol than to halve the speech coding rate, if sufficiently high SNR values can be provided in the power budget. However, in cellular systems these gains would be more modest due to increased frequency re-use distances in order to mitigate cochannel interference. The associated complexity, robustness and bandwidth efficiency ramifications are discussed in Reference 1. The lower PRMA efficiency of low-rate speech codecs is explained by the increasing dominance of the fixed header length. An interesting comparison is provided

Table 1 OVERALL PRMA SYSTEM COMPARISON

1 System	2 Modem	3 Speech rate	4 PRMA source rate	5 TDMA user bandwidth	6 Number of TDMA users/carrier	7 Number of PRMA users/carrier	8 Number of PRMA users/slot	9 PRMA user bandwidth	10 P_{perm}
		kbit/s	kbaud	kHz				kHz	
A	GMSK	13	26	20	10	17	1·70	11·8	0·6
B	GMSK	6·5	14·6	11·1	18	32	1·78	6·25	0·3
C	GMSK	3·25	8·9	6·7	30	57	1·9	3·5	0·2
D	$\pi/4$-DQPSK	13	13	16·7	12	22	1·83	9·1	0·56
E	$\pi/4$-DQPSK	6·5	7·3	9·6	22	42	1·91	4·8	0·3
F	$\pi/4$-DQPSK	3·25	4·45	5·6	36	70	1·94	2·9	0·19
G	16-StQAM	13	6·5	11·1	18	32	1·78	6·25	0·3
H	16-StQAM	6·5	3·65	6·25	32	61	1·91	3·3	0·2
J	16-StQAM	3·25	2·225	3·8	53	103	1·94	1·94	0·13

by systems B and G, both of which have identical PRMA efficiencies and bandwidth requirements, but system B comprising a quadruple complexity half-rate speech codec will be more robust against channel errors, while requiring higher supply currents. A variety of further interesting contrasts are offered by Table 1, of which perhaps the impressive bandwidth efficiency of the 16-StQAM schemes is worth mentioning, supporting 61 half-rate or 103 quarter-rate subscribers using near-future technology [7]. Lastly, when using higher slot numbers guaranteed by multilevel transmission schemes the packet dropping probability against user number curves in Fig. 1 becomes less steep, implying a more graceful grade-of-service degradation characteristic, which is an important advantage over binary modulation schemes.

Table 1 summarises the bandwidth efficiency ramifications of using an adaptive transceiver incorporating the firmware of systems A–J in a GSM channel slot. The exact definition of the system optimisation algorithms obeying different criteria requires further research [1].

15th March 1993

L. Hanzo, J. C. S. Cheung† and R. Steele (*Dept. of Electronics, University of Southampton, Southampton SO9 5NH, United Kingdom*)

† Currently with the Dept. of Electrical and Electronic Engineering, University of Bristol, United Kingdom)

References

1 STEELE, R.: 'Mobile radio communications' (Pentech Press, 1992)
2 WEBB, W., HANZO, L., and STEELE, R.: 'Bandwidth efficient QAM schemes for Rayleigh fading channels', *IEE Proc. I*, 1991, **138**, (3), pp. 169–175
3 STAPLETON, S., and COSTESCU, F. C.: 'An adaptive predistorter for a power amplifier based on adjacent channel emissions', *IEEE Trans.*, 1992, **VT-41**, (1), pp. 49–56
4 GOODMAN, D. J., and WEI, S. X.: 'Efficiency of packet reservation multiple access', *IEEE Trans.*, 1991, **VT-40**, (1), pp. 170–176
5 BACS, E., and HANZO, L.: 'A simple real-time adaptive speech detector for SCPC systems'. Proc. ICC '85, Chicago, Illinois, USA, pp. 1208–1212
6 HANZO, L., SALAMI, R. A., STEELE, R., and FORTUNE, P. M.: 'Transmission of digitally encoded speech at 1·2 kBd for PCN', *IEE Proc. I*, 1992, **139**, (4), pp. 437–447

PROCESSING OF SPECULAR ECHOES FROM PLANAR REFLECTORS IN AIRBORNE SONAR DATA

A. M. Sabatini

Indexing terms: Sonar, Robots, Ultrasonics

Airborne ultrasound sensing techniques are widely used for obtaining range information. Research is being carried out to extend the measuring capabilities of sonar ranging systems. The results of an investigation are presented aimed at understanding how a single transducer can be used for estimating the inclination angle of a specular planar reflector.

Introduction: Most of the currently used sonar ranging systems for robotic applications are based on airborne ultrasonic transducers as an inexpensive means for determining the proximity of objects. In an echo-pulse system, by far the most widely used implementation in practice, the time-of-flight (TOF) is the physical principle employed for range determination: an ultrasonic pulse is emitted and the time elapsed from transmission to reception is measured and converted to distance information, provided that the speed of sound propagation in the medium is known. Besides TOF, different acoustic signatures are being investigated in order to improve the capabilities of sonar systems without compromising their most prominent features, i.e. their relatively low cost and simplicity of implementation.

In this Letter we discuss how a single reversible transducer, that is a transducer working as a transmitter and switched after the transmission to the receiving mode to wait for reflected echoes, might tackle the problem of estimating the angle of inclination of a specular planar reflector placed at some distance from the transducer by echo amplitude information processing.

Providing a sonar with such an ability is of relevant interest for many applications in robotics: the wall-following skill, for instance, is highly desirable for mobile robotic systems or for a manipulator approaching the worktable. Owing to the poor directional properties of ultrasonic transducers, the task of predicting where the insonified target is located within the beam is usually solved by means of spatially distributed configurations of emitter/recievers for sampling the scattered field.

Physical sensor model: For a single transducer, two distinct effects are observed in the reflected echoes from tilted vertical planes in comparison to the case of a reference plane perpendicularly oriented to the transducer radiation axis:

(i) a marked attenuation of the echo amplitude, caused by the acoustic energy distribution on the radiated wavefronts

(ii) a time-spreading effect due to the finite time needed for the acoustic wavefronts to propagete across the receiving aperture.

These shaping effects on the received waveforms might be accounted for by lowpass filtering the transducer impulse frequency response $P(f)$. For a circular transducer and a planar target in the far field, that is at distances $R \gg a^2/\lambda$ (a the transducer radius, and λ the acoustic wavelength), a useful approximation to the true characteristics of this filter is provided by the Rayleigh–Sommerfeld diffraction theory [1]:

$$H(f,\theta) = \left[\cos\theta \frac{2J_1\left(\frac{2\pi a}{c} f \sin\theta\right)}{\frac{2\pi a}{c} f \sin\theta}\right]^2 \quad (1)$$

where c is the speed of sound propagation and J_1 is a Bessel function of first kind and first order. The signal geometrical attenuation, dependent on the way the acoustic wave propagates in free space, is tacitly assumed to be normalised. The acoustic signature we are interested in for inclination angle estimation is the echo amplitude peak. This signature can be theoreticaly calculated by taking the inverse Fourier transform of the function $H(f,\theta)P(f)$; for almost any practical transducer impulse response, it is approximately given by

$$A_{max} = A_0 \exp(-4\theta^2/\theta_0^2) \quad (2)$$

where θ_0 is the first null of the radiation pattern [2]:

$$\theta_0 = \arcsin\frac{0{\cdot}61\lambda}{a} \quad (3)$$

Experimental setup: For our experiments, a commercially available piezoelectric transducer (MASSA Mod. E188) with a resonance frequency of $\sim$225 kHz is used. The transducer, a flat circular disc of radius $a = 6{\cdot}5$ mm, is mounted over a rotating table at a distance $R = 20$ cm from a planar reflector. After being conditioned, the amplified echoes are digitised using a PC-compatible high-speed A/D board, with $N = 8$ bits of resolution and selectable sampling rates up to $f_s =$ 25 MHz. In Figs. 1 and 2 the transducer impulse response and the corresponding Fourier spectra are reported.

Results: Sampling rates largely in excess of the minimum allowable Nyquist frequency have been adopted (11 sample/period) to obtain adequate resolution. A typical data record is formed by $M = 650$ points. Owing to this oversampling, the largest sample of the sequence is considered to be a very good approximation of the desired echo peak amplitude value.

For large bandwidth transducers the lowpass filter effect is responsible for an apparent shift of the resonance frequency,